JOURNAL OF APPLIED ELECTROCHEMISTRY 21 (1991) 672–677

Electrodeposition of Fe–Ni–Co alloys Part I: Direct current deposition

N. H. PHAN, M. SCHWARTZ, K. NOBE*

Department of Chemical Engineering, University of California, Los Angeles, CA 90024, U.S.A.

Received 21 November 1990; revised 7 February 1991

Effects of hydrodynamic conditions, current density and solution temperature on the d.c. electrodeposition of Fe–Ni–Co alloys have been investigated with stationary planar and rotating cylindrical electrodes. The deposition rate of Fe showed mass transfer effects at cathodic potentials $\leqslant -1.35$ V/SCE. Deposition of Ni appeared to be kinetically controlled; deposition of Co appeared to be under kinetic control at potentials $\geqslant -1.35$ V/SCE but under mixed control at -1.65 V. Current efficiency of the codeposition process increased with increasing current density and decreased with increasing rotation rate. Higher solution temperatures and rotation rates extended the applied current density range where smooth, adherent, and metallic-looking deposits could be obtained. An increase in solution temperatures also decreased anomalous codeposition of Fe–Ni–Co. Calculations based on the Hessami-Tobias model provide qualitative agreement with dependence of experimental electrodeposition on applied current density, hydrodynamics and temperature.

1. Introduction

Previous work in our laboratory reported on the development of electrodeposition solutions for the iron-rich Fe–Ni alloys, Invar [1] and Super Invar [2]. The binary alloy, Invar (64% Fe, 36% Ni), and the ternary alloy, Super Invar (64% Fe, 31% Ni, 5% Co), are noted for their low thermal expansion coefficient, and commercial usage of these alloys are found where materials with this characteristic are required. Typical applications include microwave guides, spacecraft optics, laser housings and printed wired boards. This work is directed to investigating the effects of hydrodynamic conditions, temperature and applied current density on the d.c. deposition of iron-rich Fe–Ni–Co alloys.

2. Experimental details

A sulphamate-chloride solution based on previous work on d.c. deposition of binary and ternary alloys of Fe, Ni and Co was used [2]. The electrolyte solution consisted of 0.720 M nickel sulphamate, 0.266 M ferrous chloride, 0.014 M cobalt sulphamate, 0.5 M boric acid, 0.001 M (0.4 g dm^{-3}) sodium dodecyl sulphate, 0.011 M (2 g dm^{-3}) ascorbic acid, and 0.008 M (2 g dm^{-3}) saccharin with the pH adjusted to 2 with sulphamic acid.

A schematic diagram of the rotating cylindrical cathode cell has been given elsewhere [3]. The cathode was a gold plated, oxygen-free copper cylinder (0.8 cm in diameter and 0.9 cm in length), which was attached to a stainless steel shaft insulated with Teflon sleeves of slightly larger diameter. Before the electroplating, the copper cylinders were polished with 600 grit emery paper, followed by crocus cloth and finally felt cloth with alumina powder. The copper cylinders were gold plated to a thickness of 12.7 μm. After each experiment, the alloy deposit was stripped with 1:1 (v/v) HNO_3, and the gold surface was restored by replating in gold solution for about 5 to 10 min. The deposit compositions of Fe, Ni and Co were determined by analysing the HNO_3 solutions with atomic absorption spectrophotometry.

The anode (5.2 cm diameter, 2.6 cm high) was positioned co-axially to the cathode and consisted of bagged sulphur-dispersed nickel. The reference electrode was a saturated calomel electrode. Solutions were prepared from deionized-double distilled water and analytical reagent grade chemicals. Solution temperatures in the range of 26–55° C were maintained in a thermostated water bath.

3. Results

Electrodeposition of iron-rich Fe–Ni–Co alloys at applied current densities from 0.5–16 A dm^{-2} were investigated using stationary planar electrodes, non-rotating and rotating cylindrical electrodes (RCE). Experiments using RCE were operated at rotation rates from 120 (Re = 331) to 1000 r.p.m. (Re = 2764), which were within the turbulent flow regime (Reynolds number $\geqslant$ 200) [4].

Figure 1 shows that a plot of wt % Fe in the deposit vs. applied current density exhibited a maximum at 1 A dm^{-2} for a non-rotating cylindrical electrode. As will be discussed later in this paper, the maximum in iron content indicates that above this current density

* To whom correspondence should be addressed.

0021-891X/91 $03.00 + .12

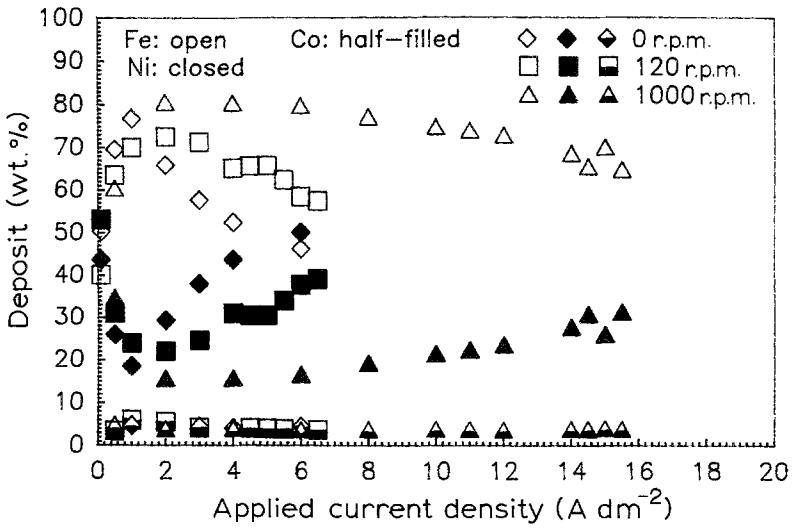

Fig. 1. Effect of rotation rate and applied current density on the metal content of deposits, 26° C.

mass transfer effects become important. The iron content in the deposit decreased from 77 to 46 wt % over the current density range of 1 to 6 A dm^{-2}. Correspondingly, the nickel content in the deposit exhibited a minimum at 1 A dm^{-2} and increased from 17 to 49 wt % as the current density increased beyond this minimum; cobalt content in the deposit changed only slightly.

For rotating electrodes, plots of wt % Fe against current density also exhibited maxima which shifted to higher current densities with increasing rotation rate (Fig. 1). Andricacos *et al.* [5] found similar behaviour with rotating disc electrodes in dilute solutions of Fe/Ni (0.005 M ferrous chloride and 0.2 M nickel chloride.)

Over the entire applied current density range studied, the Fe content of the deposits was dependent on the rotation rate. Prior to the maxima in deposit Fe content, an increase in rotation rate decreased the Fe content; this decrease with increasing rotation rate occurred over a rather narrow current density range ($\leqslant$ 1 A dm^{-2}). At higher current densities, an increase in rotation rate increased the Fe content. The wt % Ni against applied current density plots exhibited minima with Ni content decreasing as rotation rates increased at higher applied current densities. On the other hand, the Co content fluctuated between 3 to 6% over the current density range from 0–6 A dm^{-2}. Above 6 A dm^{-2}, the Co content leveled off at 3.5% and was relatively independent of applied current density.

At a given rotation rate, there was a critical current density above which deposits tended to crack or become burnt, powdery and nonmetallic in appearance; experiments were terminated at this point. This critical current density was dependent on rotation rate. For example, an increase in rotation rate from 0 to 1000 r.p.m. increased this critical current density from 6 to 16 A dm^{-2}, as shown in Fig. 1.

Partial current densities of Fe, Ni and Co were determined from their respective measured deposit contents and the time duration of the deposition experiments (in each case, 60 coulombs were passed). The partial current density–applied current density behaviour at 120 and 1000 r.p.m. is presented in Fig. 2. It is shown that at higher applied current densities an increase in rotation rate increased the rate of deposition of iron (i_{Fe}). This is due to significant mass transfer effects in the deposition rate of iron, as mentioned above. Since deposits produced at higher current densities ($>$ 16 A dm^{-2}) were powdery and non-adherent, which precluded analysis of the deposit

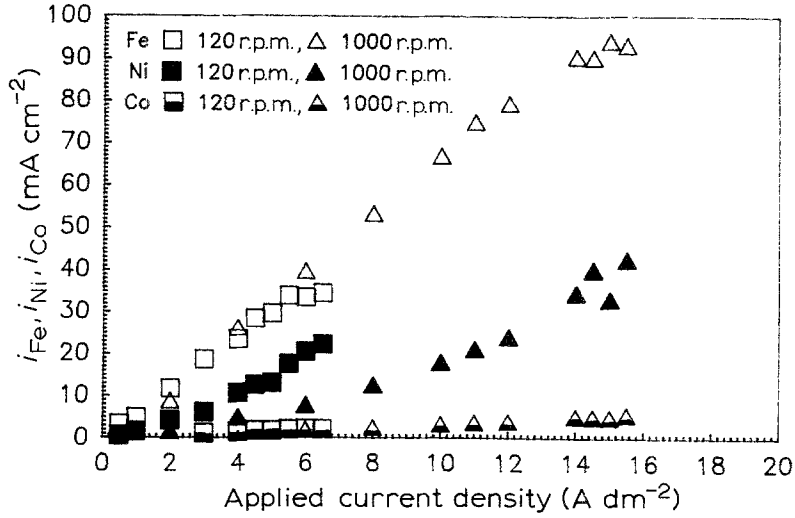

Fig. 2. Effect of rotation rate and applied current density on partial current densities, 26° C.

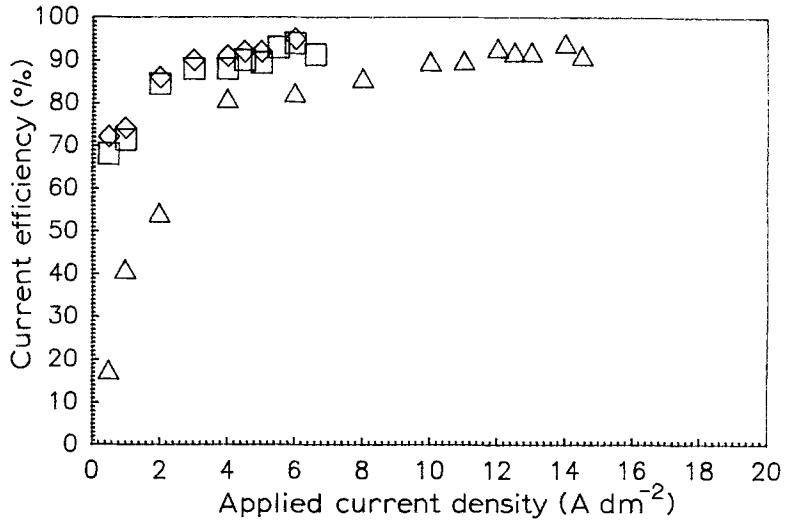

Fig. 3. Effect of rotation rate and applied current density on the current efficiency of the electrodeposition of Fe–Ni–Co alloys, 26° C. (◇) 0, (□) 120 and (△) 1000 r.p.m.

composition, limiting partial current densities of iron could not be obtained (Fig. 2).

According to Andricacos et al. [5], an increase in the rotation rate of rotating disc electrodes shifted the nickel deposition potentials toward more cathodic values. Consequently, Ni partial current density should decrease with increasing rotation rate as also indicated in the experimental results shown in Fig. 2. There was little dependence of the partial current density of Co on rotation rate.

Although increased rotation rates extended the applied current density range wherein better quality deposits were produced, the current efficiency decreased with increasing rotation rate (Fig. 3). This is in agreement with Dahms and Croll's observation of strong mass transfer effects on the rate of hydrogen evolution during co-deposition of Fe and Ni [6]. Therefore, an increase in rotation rate should increase the rate of hydrogen evolution, and the total current efficiency for metal deposition should then be lowered. Andricacos *et al.* also reported strong mass transfer effects on the hydrogen evolution rate during co-deposition of Fe and Ni [5].

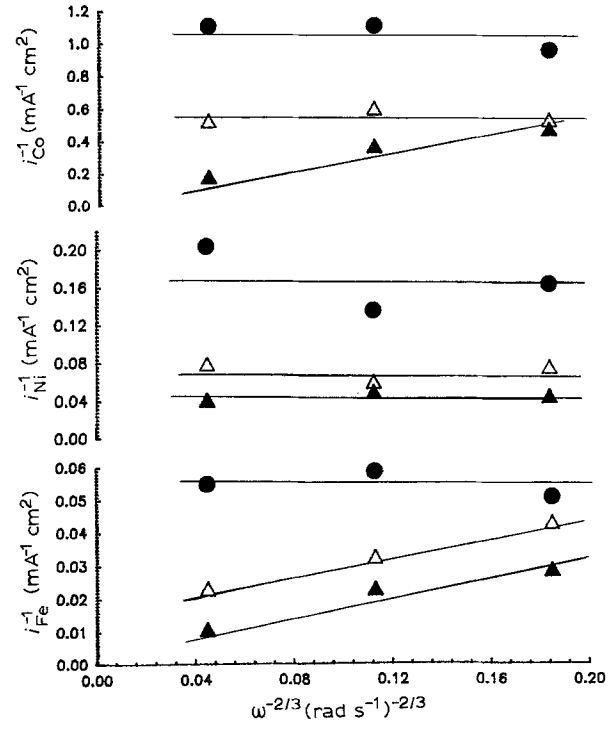

Fig. 4. Reciprocal partial current densities against (rotation rate)$^{-2/3}$ plots, 26° C. E: (●) −1.20, (△) −1.35 and (▲) −1.65 V.

Figure 4 presents plots of the reciprocal of partial current densities of Fe, Ni, and Co and $\omega^{-2/3}$. At lower cathodic potentials (low deposition rate), i_{Fe}^{-1} was independent of rotation rate, but at relatively higher cathodic potentials (higher applied current densities) of −1.35 V and −1.65 V/SCE, i_{Fe}^{-1} increased linearly with increase in the reciprocal of the rotation rate to the 2/3 power. Since mass transfer rates at a rotating cylinder in the turbulent flow regime vary as $\omega^{2/3}$, the results in Fig. 4 clearly indicate that there were strong mass transfer effects on Fe codeposition for cathodic potentials < -1.20 V/SCE (this corresponds to the applied current densities at the maxima in Fig. 1). On the other hand, the partial current densities of Ni were independent of rotation rate for cathodic potentials down to −1.65 V/SCE. Therefore, it is concluded that the codeposition of Ni was kinetically controlled in the applied current density range investigated. Plots of $1/i_{Co}$ against $\omega^{-2/3}$ were independent of rotation rate at low cathodic potentials (low applied current densities), but mass transfer effects were evident at −1.65 V/SCE as i_{Co}^{-1} increased linearly with $\omega^{-2/3}$.

Since solution temperatures affect the rates of metal deposition, temperatures from 26 to 55° C were studied with stationary planar and rotating cylindrical electrodes at 1000 r.p.m. Figure 5 shows that at 1000 rpm an increase in temperature from 26 to 55° C decreased the Fe content of the deposits and increased the Ni content of the deposits. At 26° C (see Fig. 6), the rate of deposition of Fe was always higher than that of Ni even though Ni^{2+} was present at a much higher solution concentration. However, at 55° C there was a certain current density (56 A dm^{-2}) above which the rate of deposition of Ni became greater than iron.

As shown in Fig. 7 for stationary planar electrodes, linear Arrhenius plots of the partial current densities of Ni and Co (at 1.5 A dm^{-2}) were obtained; the partial current density of Fe was independent of temperature. From the slopes of the linear regression lines

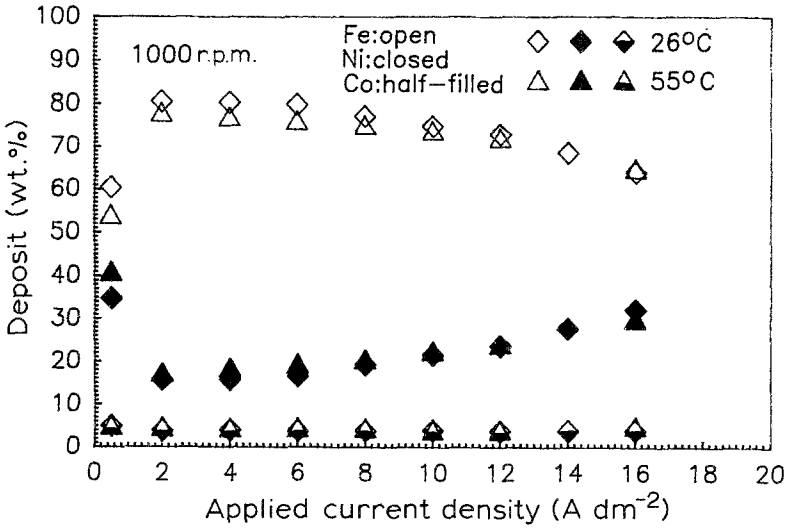

Fig. 5. Effect of temperature on the metal content of deposits at various applied current densities, 1000 r.p.m.

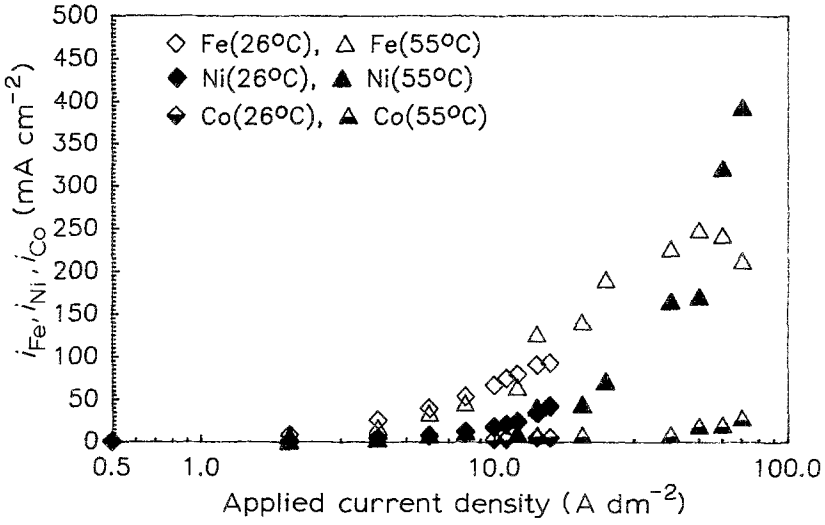

Fig. 6. Effect of temperature on partial current densities at various applied current densities, 1000 r.p.m.

correlating the Ni and Co data in Figure 7, the apparent activation energies were calculated as 28.2 and 14.3 kJ mol^{-1}, respectively.

The 'selectivity ratio' of Fe/Ni and Co/Ni is defined as the molar ratio of Fe/Ni or Co/Ni in the deposit to the molar ratio of Fe/Ni or Co/Ni in the solution. As temperatures increased from 26 to 55° C (see Fig. 8) at an applied current density of 2 A dm^{-2}, the 'selectivity ratio' of Fe/Ni decreased from about 14 to 10 indicating that the codeposition of Fe–Ni was less anomalous at higher solution temperatures. Similarly, the 'selectivity ratios' of Co/Ni decreased from about 12 to 9 with increase in temperature from 26 to 55° C. In a previous study of the electrodeposition of binary alloys of Fe, Ni and Co, Fe–Co codeposition was the least anomalous, Co–Ni was the most anomalous and Fe–Ni was intermediate [2].

Figure 8 shows that the 'selectivity ratios' of Fe/Ni

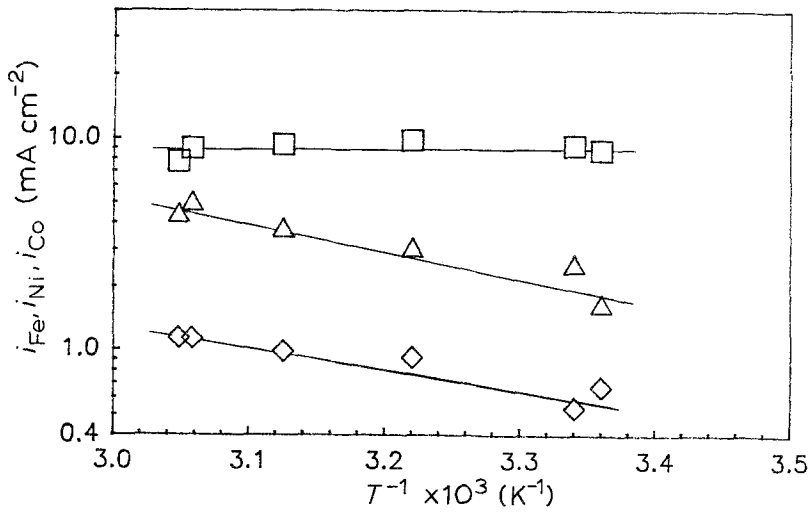

Fig. 7. Arrhenius plots of partial current densities, applied current density of 1 A dm^{-2}; stationary planar electrodes. (□) Fe, (△) Ni and (◇) Co.

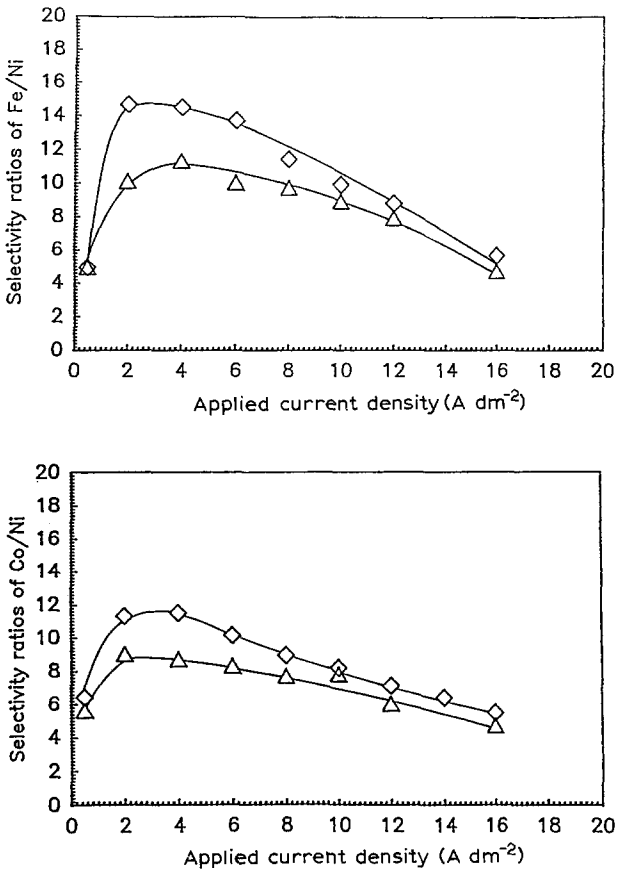

Fig. 8. Effect of temperature on the selectivity ratios of Fe/Ni and Co/Ni, 1000 r.p.m. (a) Fe/Ni (◇) 26° C and (△) 55° C; (b) Co/Ni (◇) 26° C and (△) 55° C.

and Co/Ni reached a maximum at low applied current density and then decreased with increase in current density. At the current densities of this maximum the codeposition of Fe–Ni and Co–Ni was most anomalous. Beyond this point, codeposition became less anomalous as the applied current density increased. Since the magnitudes of these ratios were lower at higher solution temperatures, the degree of anomalous codeposition of Fe/Ni and Co/Ni in solutions containing all three metal species decreased with increase in temperature.

4. Discussion

The experimental results provided the following observations of the electrodeposition of iron-rich Fe–Ni–Co ternary alloys:

1. A maximum in the wt % Fe–applied current density plots occurred with a corresponding minimum in similar plots for nickel; dependence of wt % Co on applied current density was not appreciable.

2. At applied current densities greater than at the maximum wt % Fe, higher rotation rates resulted in larger deposit Fe content.

3. At applied current densities greater than at the maximum wt % Fe, the deposit Fe content decreased as the current density increased.

4. The deposit Fe content was lower at higher temperatures. That is, less anomalous deposition.

After these experiments were completed, an interesting model was published to explain the electrodeposition behaviour of the nickel-rich Fe–Ni alloy, Permalloy [7]. Computer calculations were presented that were in good agreement with experimental results published earlier [5]. The key feature of the Hessami-Tobias model is the hypothesis that electrodeposition of Ni and Fe occurs not only from Ni^{2+} and Fe^{2+} but also from the Ni and Fe hydroxide ions, $NiOH^+$ and $FeOH^+$, respectively, with larger rate constants for the deposition of the metal hydroxide ions than the free ions. Since the pH at the cathode increases during electrodeposition of Fe and Ni due to hydrogen evolution, the surface concentrations of $FeOH^+$ and $NiOH^+$ would be higher than obtained at the bulk pH. Since the dissociation constant of $FeOH^+$ selected by Hessami and Tobias [7] was three orders of magnitude lower than $NiOH^+$, surface concentrations of the former would be so much larger than the latter. Based on this model, a good conceptualization of anomalous deposition of Permalloy was achieved.

A rough approximate calculation procedure will be used to assess the applicability of the H–T model [7] to the present experimental results of iron-rich Fe–Ni–Co alloys. The pH at the rotating cylindrical cathode was estimated as follows:

$$i_H^\omega = nFk_m^\omega([H^+]_b - [H^+]_s^\omega) \quad (1)$$

where i_H^ω = rate of hydrogen ion discharge at rotation rate ω; k_m^ω = mass transfer coefficient at a specific ω, $[H^+]_b$ = bulk hydrogen ion concentration, and $[H^+]_s^\omega$ = surface hydrogen ion concentration at a specific ω. $[H^+]_s^\omega$ was then related to corresponding values at a stationary electrode with Equation 1,

$$[H^+]_s^\omega = [H^+]_b - \frac{\delta_\omega}{\delta_0}\frac{i_H^\omega}{i_H^0}([H^+]_b - [H^+]_s^0) \quad (2)$$

Romankiw's surface pH values obtained from experiments with stationary electrodes [8] were used for $[H^+]_s^0$. The hydrogen ion discharge rates at ω and $\omega = 0$ were determined from experimental data. The diffusion layer thickness at $\omega = 0$ was approximated as 0.03 cm and at ω was determined by a modified form of the correlation given by Eisenberg *et al.* for rotating cylinders [9],

$$Sh = \frac{k_m d}{D_i} = 0.0791 Re^{2/3} Sc^{1/3} \quad (3)$$

where d = cylinder diameter, D_i = diffusion coefficient of species i, $Re = d^2\omega/2\nu$, $Sc = \nu/D_i$ and ν = kinematic viscosity of the solution. The surface concentration of Fe^{2+} at ω is estimated by

$$[Fe^{2+}]_s^\omega = [Fe^{2+}]_b - \frac{i_{Fe}\delta_\omega}{2FD_{Fe^{2+}}} \quad (4)$$

Based on the results given in Fig. 4,

$$[Ni^{2+}]_s = [Ni^{2+}]_b \quad (5)$$

Values for $[OH^-]_s^\omega$ were determined from $[H^+]_s^\omega$ values. Then, $[Fe^{2+}]_s^\omega$, $[Ni^{2+}]_s$ and $[OH^-]_s^\omega$ were used

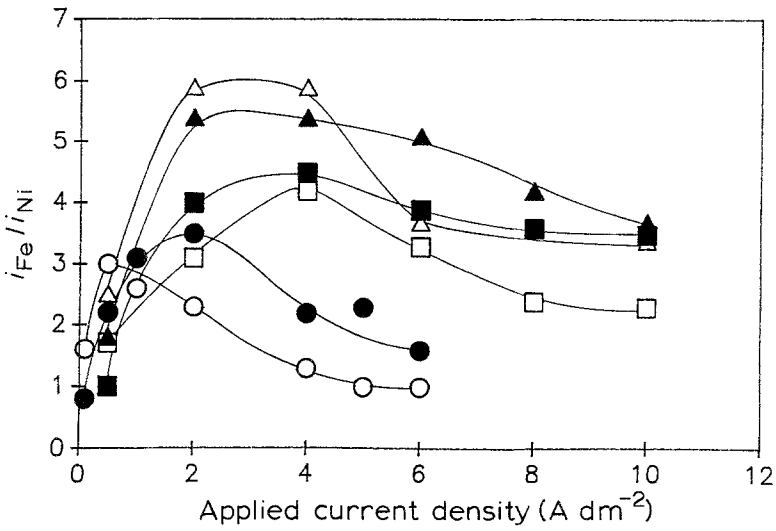

Fig. 9. Comparison of experimental and calculated i_{Fe}/i_{Ni} ratios as a function of applied current density, rotation rate and temperature. (○) 26° C, 120 r.p.m., (△) 26° C, 1000 r.p.m., and (□) 55° C, 1000 r.p.m. Experimental: filled points; calculated: open points.

to estimate $[FeOH^+]_s^\omega$ and $[NiOH^+]_s^\omega$ from Equations 6 and 7,

$$[FeOH^+]_s^\omega = K_{FeOH^+}[OH^-]_s^\omega[Fe^{2+}]_s^\omega \quad (6)$$

$$[NiOH^+]_s^\omega = K_{NiOH^+}[OH^-]_s^\omega[Ni^{2+}]_s \quad (7)$$

The ratio of the partial currents for Fe and Ni can be expressed as

$$\frac{i_{Fe}}{i_{Ni}} = (k_{Fe^{2+}}[Fe^{2+}]_s^\omega \exp \alpha_{Fe^{2+}} FE/RT + k_{FeOH^+}[FeOH^+]_s^\omega \exp \alpha_{FeOH^+} FE/RT)/ \times (k_{Ni^{2+}}[Ni^{2+}]_s \exp \alpha_{Ni^{2+}} FE/RT + k_{NiOH^+}[NiOH^+]_s^\omega \exp \alpha_{NiOH^+} FE/RT) \quad (8)$$

Equation 8, and the equilibrium constants and kinetic parameters provided by Hessami and Tobias [7], except for slightly modified values of $k_{Fe^{2+}}$ and k_{FeOH^+} ($k_{Fe^{2+}} = 0.4k_{Fe^{2+}}^{H-T}$ and $k_{FeOH^+} = 0.4k_{FeOH^+}^{H-T}$) to account for the presence of organic additives, were used to calculate i_{Fe}/i_{Ni} values at 26° C and various i_{appl} and ω. At 55° C, equilibrium constants (including the ionization constant of water) were determined from data in NBS tables [10]; activation energies for the rate constants of Fe^{2+}, $FeOH^+$, Ni^{2+} and $NiOH^+$ were assumed to be equivalent. Experimental results and the calculations of i_{Fe}/i_{Ni} values as a function of applied current density at 26° C, and 120 and 1000 r.p.m., and at 55° C and 1000 r.p.m. are compared in Fig. 9. The calculated dependence of i_{Fe}/i_{Ni} on applied current density and rotation rate are shown to be in qualitative agreement with the experimental results. Both show clearly that anomalous deposition of Fe and Ni from the ternary metal plating solution is less at higher temperatures.

Acknowledgment

This work was initiated by a subcontract under Department of Energy Prime W-7405-Eng-48 at Lawrence Livermore National Laboratory. The assistance of Jack Dini of LLNL is appreciated. The graphics were ably done by Brian Kelvin Nobe with some assistance from Ronald Perez.

References

[1] D. L. Grimmett, M. Schwartz and K. Nobe, *Plat. Surf. Fin.* **75** (June 1988) 94.
[2] N. H. Phan, M. Schwartz and K. Nobe, *ibid.* **75** (Aug. 1988) 46.
[3] N. H. Phan, Dissertation, UCLA, June 1990.
[4] J. S. Newman, 'Electrochemical Systems', Prentice Hall, Englewood Cliffs, New Jersey (1973).
[5] P. C. Andricacos, C. Arana, J. Tabib, J. Dukovic and L. T. Romankiw, *J. Electrochem. Soc.* **136** (1989) 1336.
[6] H. Dahms and I. M. Croll, *ibid.* **112** (1965) 771.
[7] S. Hessami and C. W. Tobias, *ibid.* **136** (1989) 4611.
[8] L. T. Romankiw, Proceedings of the Symposium on Electrodeposition Technology, Theory and Practice, 301, Electrochem. Society, Pennington, NJ (1987).
[9] M. Eisenberg, C. W. Tobias and C. R. Wilke, *J. Electrochem. Soc.* **101** (1954) 306.
[10] NBS Tables of Chemical Thermodynamic Properties, Physics & Chemistry Reference Data, Washington D.C., **11**, Suppl. 2 (1982).